INDONESIAN JOURNAL ON GEOSCIENCE
Geological Agency
Ministry of Energy and Mineral Resources

Journal homepage: http://ijog.geologi.esdm.go.id
ISSN 2355-9314, e-ISSN 2355-9306

Geochemical Characteristics of Limestone of Wonosari-Punung Formation, Gunungkidul Regency, Yogyakarta, Indonesia

Didik Dwi Atmoko, Anastasia Dewi Titisari, and Arifudin Idrus

Department of Geological Engineering, Faculty of Engineering, Universitas Gadjah Mada
Jln. Grafika No. 2, Bulaksumur, Yogyakarta 55281, Indonesia

Corresponding author: adtitisari@gmail.com

Manuscript received: July 6, 2017; revised: August 30, 2017;
approved: April 26, 2018; available online: August 27, 2018

Abstract - A geochemical study was carried out to determine the geochemical characteristics of limestone in Wonosari-Punung Formation, and to suggest its depositional conditions and the source of rare earth elements. The study was conducted at Ponjong Area, Gunungkidul Regency, Daerah Istimewa Yogyakarta, Indonesia. White limestone which contains more abundant calcite is characterized by the highest CaO concentration. Red limestone which is associated with impure minerals such as siderite, rodochrosite, hematite, and titanite is typified by depleted CaO but higher SiO_2, Fe_2O_3, MnO, and TiO_2 concentrations. Grey limestone characterized by depleted CaO and higher MnO contents is considered to be influenced by the presence of impure minerals of manganite ($Mn_2O_3.H_2O$) and/or pyrolusite (MnO_2). Depletion of Sr concentration in the coloured limestone indicates that the diagenetic process increases from the white limestone to the coloured limestone. The process possibly occurred post-deposition of the limestones. The limestones show positive Mn* values (2.46 - 2.95) and authigenic U values (0.89 - 3.38) that suggest an oxidative environment. The Ce/Ce* values (0.57 - 0.80), Eu/Eu* values (1.04 - 1.88), high Y/Ho ratio, and low La_N/Yb_N ratio are indications that the rare earth elements in the limestones were derived from terrigenous materials. The positive Eu anomaly and enrichment of Cr and Mn of the limestones are indications of hydrothermal fluid activity taking place in the studied area. Based on the geochemical characteristics of the Punung-Wonosari limestones, the depositional environment and the source of rare earth elements of the limestones were therefore influenced by a combination of hydrothermal fluid activity with small amount of terrigenous material input and post depositional diagenetic process.

Keywords: diagenetic process, rare earth elements, trace elements, oxidative condition, source of rare earth elements

How to cite this article:

Atmoko, D.D., Titisari, A.D., and Idrus, A., 2018. Geochemical Characteristics of Limestone of Wonosari-Punung Formation, Gunungkidul Regency, Yogyakarta, Indonesia. *Indonesian Journal on Geoscience*, 5 (2), p.179-197. DOI: 10.17014/ijog.5.2.179-197

INTRODUCTION

Background

Wonosari-Punung Formation is a Miocene limestone formation located in the Southern Mountain Basin. Toha *et al*. (1994) mentioned that Wonosari-Punung Formation mainly consists of bedding and reefal limestones. Several geological studies have been carried out on Wonosari-Punung Formation such as the development of the Miocene Wonosari-Punung Formation (Lokier, 1999), reef facies of Wonosari-Punung Formation (Siregar *et al*., 2004), sequence stratigraphy and diagenesis of carbonate rocks of Wonosari-Punung Formation (Jauhari and Toha, 2005), depositional environment of carbonate rocks of Wonosari-Punung Formation in eastern Pacitan (Mukti *et al*., 2005), Punung paleoreef (Premonowati *et al*., 2012), and a geochemical study of major oxide compound on Ponjong limestone (Atmoko *et al*., 2016). Most of the previous studies are based on outcrop determination, petrographic and paleontological analyses, except the study of Atmoko *et al*. (2016) that more focused on a geochemical study. The studies were not emphasized on limestone geochemical research of Wonosari-Punung Formation which was the subject of this study, although studies of limestone geochemistry are very important to understand the depositional condition of a limestone formation. Previous geochemical studies that have been carried out in some places in the world and show the important things of geochemical research for interpretation of limestone depositional condition among others are oceanic chemistry of the rare earth elements (Elderfield, 1988), geochemistry of Cauvery Basin, southeastern India and its implication to the provenance of limestone (Madhavaraju and Lee, 2009), rare earth elements in limestones of Kallankurichchi Formation, Tamil (Madhavaraju and Ramasamy, 1999), the source of rare earth elements in carbonate strata of the Aptian-Albian Mural Formation, Mexico, related to hydrothermal fluid effect (Madhavaraju and Gonzáles-León, 2012), depositional conditions in limestone correlated with paleo-redox condition, paleogeography and proximity to the source area (Liu *et al*., 1988; German and Elderfield, 1990; Holser, 1997; Northdurft *et al*.,2004; Lawrence and Kamber, 2006; Madhavaraju and Gonzáles-León, 2012). According to the previous geochemical studies, some elements such as Sr and Mn are diagenetic indicators because of their widely divergent partition coefficients, their acceptance into the carbonate lattice, and their large compositional differences in marine and meteoric water (Bodine *et al*., 1965; Turekian, 1972). Negative Ce anomalies preserved in carbonate sediments and rocks are a strong indication that the rocks are precipitated in an oxide environment (Tostevin *et al*., 2016). Cerium anomalies can also be used as a potential indicator for eustatic sea-level (Chen *et al*., 2012). A positive Eu anomaly in a limestone formation is an indicator of hydrothermal solutions effect on limestone (*e.g*. German *et al*., 1993; Kurian *et al*., 2008). In this study, geochemical characteristics of the limestone on Wonosari-Punung limestone formation will be determined based on geochemical elements, *e.g*. major oxide compounds (SiO_2, Al_2O_3, Fe_2O_3, CaO, MgO, K_2O, Na_2O, MnO, TiO_2, and P_2O), trace elements (Cr, Mn, Fe, Rb, Sr, Y, Zr, Nb, Ba, La, Ce, and Eu), and rare earth elements contained in the Wonosari-Punung limestone. This geochemical characteristic of Wonosari-Punung limestone can be used for interpretation of its depositional conditions and its source of rare earth elements. Furthermore, it is also possible for interpreting sea level changes of the limestone depositional environment. Therefore, this study might be useful for better reconstruction and understanding the depositional environment of the Wonosari-Punung Formation. This study was conducted at Ponjong Area, Gunungkidul Regency, Daerah Istimewa Yogyakarta, Indonesia (Figure 1).

Geological Settings

By referring to the regional geological map of the Surakarta-Giritontro Quadrangle, Java, scale 1:100,000 (Surono *et al*.,1992), the studied area is composed of Semilir Formation and Wonosari-Punung Formation (Figure 1a). The Wonosari-Punung Formation consists of limestone, marly-tuffaceous limestone, conglomeratic limestone, tuffaceous sandstone, and siltstone. It was deposited unconformably on the Semilir Formation comprising tuff, dacitic pumice breccia, tuffaceous sandstone, and shale (Surono *et al*. 1992). According to Atmoko (2016), the studied area is dominated by limestone units that belong to the Wonosari-Punung Formation (Figures 1), and an older unit of tuffaceous sandstone-calcareous sandstone which distributes on north-west and north-east of the studied area, considered to be a member of the Semilir Formation (Figure 1).

A previous study conducted by Atmoko (2016) shows four types of limestone in the studied area composed of molluscan packstone, coralline rudstone, foraminiferal grainstone, and coralline framestone-bafflestone (Figure 1b). Atmoko (2016) explains that the limestone in the studied area was deposited in a reef depositional environment and formed a reef system. Geological

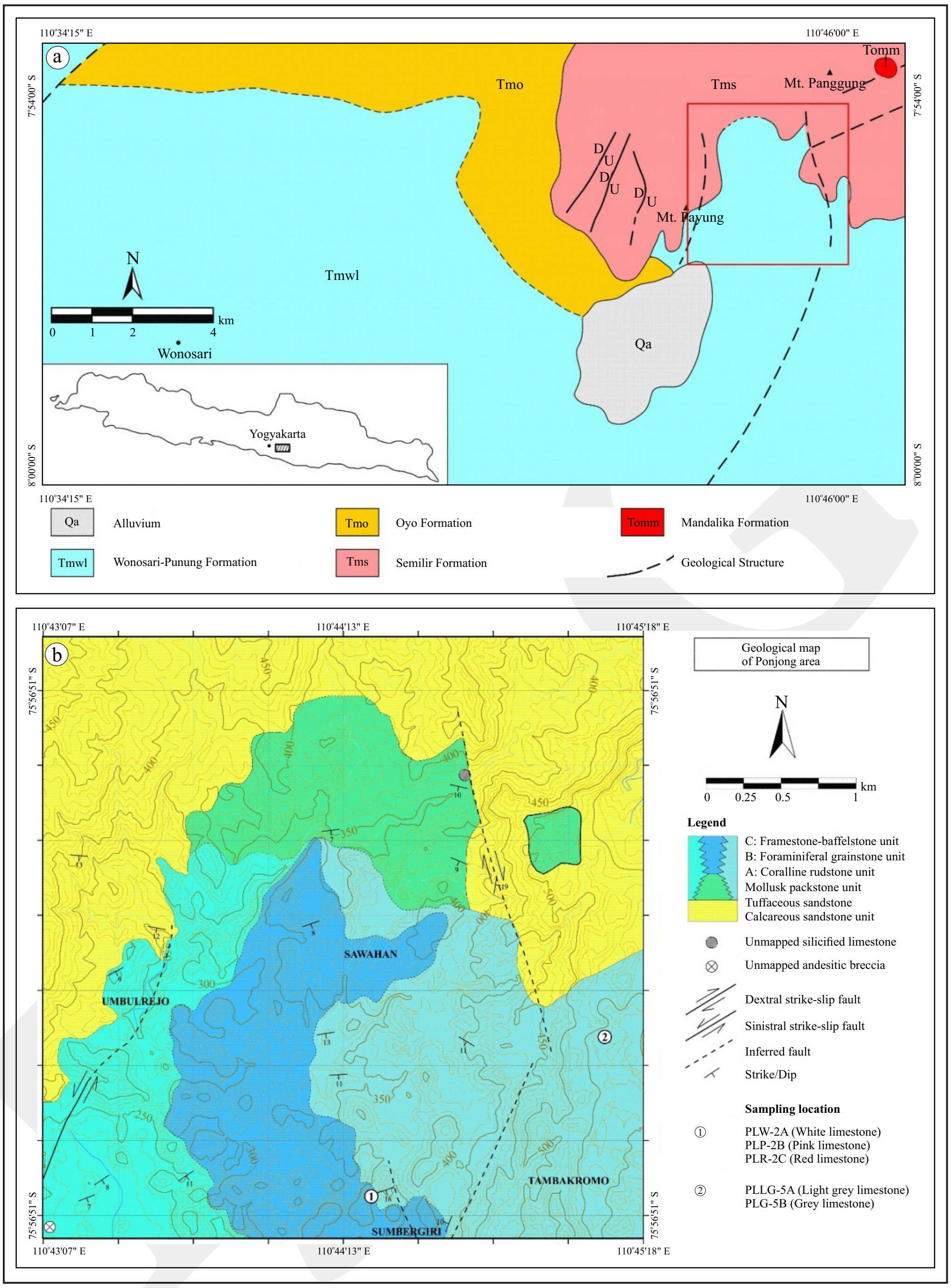

Figure 1. a. Regional geological map of the central-southern part of the geological map of Surakarta-Giritontro Quadrangle (simplified from Surono *et al*., 1992) and the location of the studied area (noted: open red square); b. Geological map of the Ponjong area (modified from Atmoko, 2016) showing the distribution of lithology units in the studied area and the sampling location for this study.

structures which develop in western and eastern parts of the studied area are strike-slip faults (Atmoko, 2016). Unmapped silicified limestone is distributed at the northeastern part of the studied area and is associated with the NW-SE fault (Figure 1b).

Material and Methods

The rock sample collecting for this study was not carried out from a measuring section, but the outcrop sampling was based on the colour difference of the limestone. Considering Atmoko

(2016), the limestone has been deposited in a reef depositional environment which formed a reef system. Consequently, the measuring section for the sampling was not available to be conducted because of difficulty on finding limestone bedding in the studied area. Representative samples for this study were collected in locations that were shown in Figure 1b. The limestone in samples of the studied area has five colour variations, those are white (PLW-2A), pink (PLP-2B), red (PLR-2C), light grey (PLLG-5A), and grey (PLG-5B). However, the colours are simplified into white, red, and grey ones. The geochemistry analysis using ICP-AES and ICP-MS of major oxide and trace elements including rare earth elements, respectively are performed on these five samples to know their geochemical characterization.

The preparation method and analytical procedures of ICP-AES for the samples of this study were using standard techniques described by Liberatore (1994). Each prepared limestone sample (0.100 g) was added to lithium metaborate/lithium tetraborate flux, mixed well and fused in a furnace at 1,000°C. The result was then cooled and dissolved in 100 ml of 4% nitric acid/2% hydrochloric acid. This solution was then analyzed by ICP-AES (Inductively Coupled Plasma - Atomic Emission Spectroscopy) that was conducted in Laboratory of ALS Canada Ltd., in North Vancouver, Canada. The results were then corrected for spectral inter-element interference. Four certified reference materials: SRM88B, SY-4, AMIS0085, and AMIS0167 were measured using the same procedure as the samples and were used in data calibration. The loss in ignition (LOI) was analyzed using the gravimetric method. Each prepared limestone sample (1.0 g) was placed in an oven at 1,000°C for one hour, cooled, and then weighed. The totally thirty-three trace elements including rare earth elements analysis, each prepared limestone sample (0.100 g) were added to lithium metaborate/ lithium tetraborate flux, mixed well and fused in a furnace at 1,025°C. The result was then cooled and dissolved in an acid mixture containing nitric, hydrochloric, and hydrofluoric acids. This solution was then analyzed by ICP-MS (Inductively Coupled Plasma - Mass Spectrometry) that was also performed in the Laboratory of ALS Canada Ltd. The analytical procedures were similar to those described in a previous study (Chien *et al*., 2006). The sample standard of OREAS-105, SRM88B, AMIS0085, and AMIS0304 were analyzed as unknown samples to check the long term accuracy and reproductibility for the limestone samples. This study used additional major oxide data from Menezes (2015) who performed the major element analysis using XRF (X Ray Fluorescence) on limestone of Wonosari-Punung Formation in Ponjong Area. Note that Menezes (2015) did not perform trace element data.

Values of normalization for plotting trace element concentration of the limestone samples are from Average Phanerozoic Limestone (Condie *et al*., 1991), whilst PAAS (Post-Archean Australian Shale) normalization (Guimaraes *et al*., 2013) is used for plotting major oxide and rare earth element (REE) concentrations of the samples.

RESULT AND DISCUSSION

Geochemically, enrichment of some major oxide concentrations such as Fe_2O_3 and TiO_2 shown on Table 1, indicates increasing colour gradation from white to pink then to red limestones. On the other hand, increasing MnO concentration reflects the rise of changing colour from white to light grey, then to grey limestones. Therefore, pink limestone is considered as a colour transition between white limestone and the red one; and light grey limestone reveals as a colour gradation from white limestone to grey limestone. Based on the colour of limestone, in the studied area, there are five collected limestone samples for this study which are white (PLW-2A), pink (PLP-2B), red (PLR-2C), light grey (PLLG-5A), and grey (PLG-5B). The photographs of colour variety of the representative limestone samples are shown in Figure 2.

Table 1. Major Oxide Concentration (wt%) in Limestone of Wonosari-Punung Formation, Ponjong Area, Gunungkidul Regency, Daerah Istimewa Yogyakarta

Rock	**White Limestone**		**Pink Limestone**		**Red Limestone**		**Light Grey Limestone**				**Grey Limestone**			
Reference	**This Study**	**Menezes (2015)**	**This Study**	**Menezes (2015)**	**This Study**	**Menezes (2015)**	**This Study**	**Menezes (2015)**	**Menezes (2015)**	**This Study**	**Menezes (2015)**	**Menezes (2015)**	**Menezes (2015)**	**Menezes (2015)**
Sample No	**PLW-2A**	**AMBM-40**	**PLP-2B**	**AMBM-13**	**PLR-2C**	**AMBM-48**	**PLLG-5A**	**AMBM-11**	**AMBM-93**	**PLG-5B**	**AMBM-1.A**	**AMBM-1.B2**	**AMBM-3.A**	**AMBM-3.B**
SiO_2	0.61	0.755	0.81	1.93	1.7	3.35	1.36	2.157	1.37	0.74	1.23	0.713	0.994	2.431
Al_2O_3	0.19	0.307	0.31	0.514	0.89	1.691	0.44	0.836	0.502	0.25	0.922	0.537	0.727	1.404
Fe_2O_3	0.1	0.125	0.16	0.819	0.51	0.648	0.26	0.649	0.264	0.19	0.418	0.298	0.359	0.892
CaO	54	54.84	54	52.01	53.1	51.48	54	52.17	54.12	53.1	51.57	53.68	53.5	50.37
MgO	0.29	0.71	0.31	0.456	0.31	1.195	0.3	0.836	0.562	0.22	0.674	0.585	0.62	0.754
K_2O	0.01	0.021	0.01	0.011	0.02	0.084	<0.01	2.75	0.019	<0.01	0.034	0.029	0.036	0.051
Na_2O	0.04	1.363	0.04	2.441	0.04	2.62	0.03	BDL	1.769	0.01	2.97	2.71	2.78	3.16
MnO	<0.01	0.033	0.01	0.736	0.01	0.04	0.48	0.496	0.052	0.61	8.713	4.213	4.519	9.186
TiO_2	0.01	0.012	0.01	0.023	0.04	0.082	0.02	0.011	0.02	0.01	<0.00034	0.008	0.007	0.017
P_2O_5	<0.01	<0.00069	0.01	0.135	0.01	<0.00069	0.02	0.374	<0.00069	0.02	0.007	<0.00069	<0.00069	0.018
LOI	43.2	-	43.1	42.89	42.7	-	42.6	-	42.94	42.9	-	-	-	-

Explanation: <0.01 below detection limit of this study analysis
BDL, <0.00034, and <0.00069 below detection limit of Menezes (2015) analysis

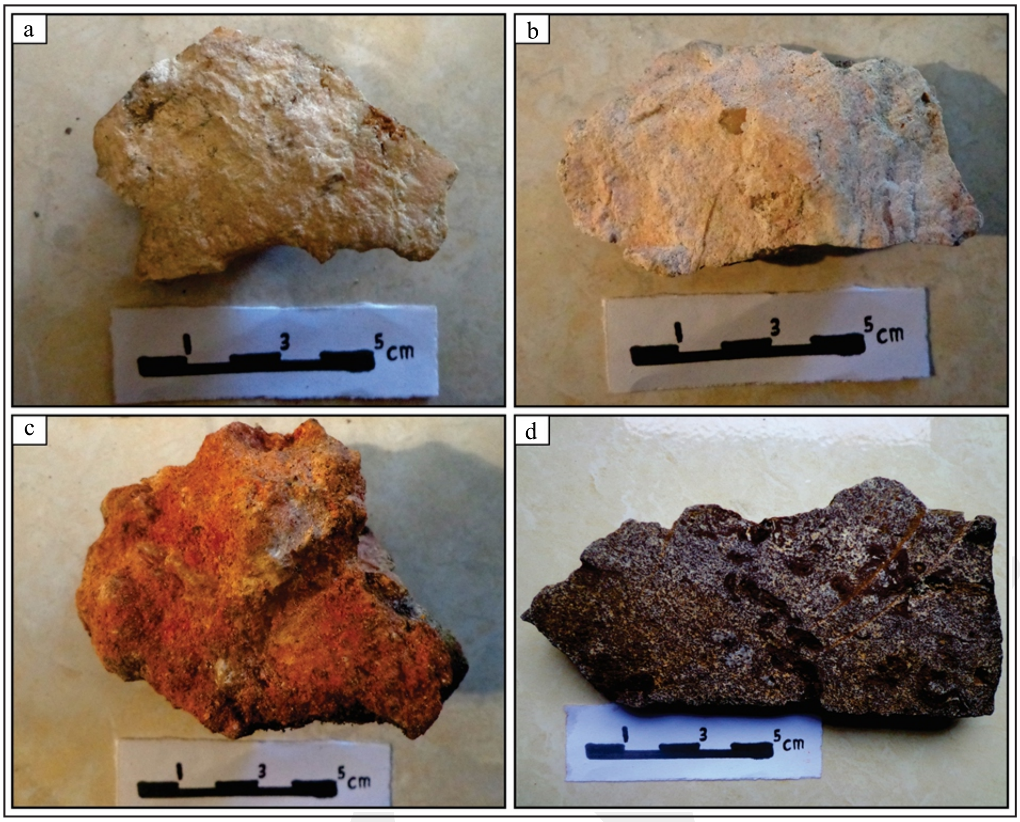

Figure 2. Hand specimen photographs of Ponjong limestone of the Wonosari-Punung Formation. a). White limestone; b). Pink limestone; c). Red Limestone; d). Grey limestone.

Petrography observation of limestone samples PLW-2A, PLR-2C, and PLG-5B are shown on Figures 3a-f, respectively. The results of geochemical analysis (major oxide concentration and trace element concentration) of the limestone samples are shown in Tables 1 and 2. Furthermore, Table 3 shows the result of normative mineralogical calculation of the limestone samples. The mineralogical calculation refers to a normative calculation for sedimentary rocks according to Medrano and Piper (1992). Generally, petrographic identification of the limestone samples exhibits almost similar petrographic characteristics, and they can be termed as packstone foraminifera-algae by referring to the classification of Embry and Klovan (1971). However, the petrographic mineral identification demonstrates differences in mineral compositions of them. The identifications are consistent with a normative mineralogical calculation of the limestone samples (Table 3). The white limestone which is dominated by calcite mineral forming grains of foraminifera and algae, and the matrix (Figures 3a and 3b) consists of 95.48 wt. % of calcite mineral which is the highest calcite mineral of all of the limestone samples (Table 3). The red limestone indicates calcite as the main mineral (93.07 wt.%) in the forming of foraminifera, algae, and matrix, and the presence of mineral quartz, feldspar (plagioclase), and hematite is in very small quantities of 2.24 wt.%, 2.50 wt.%, and 0.51 wt.%, respectively (Figures 3c and 3d, and Table 3). Indication of pyrolusite and or manganite impurity minerals (0.75 wt. %) in very small amounts are presented in the grey limestone (Figures 3e and 3f, and Table 3).

The major oxide data in Table 1 show that limestone of Wonosari-Punung Formation contains CaO concentration that ranges from 50.37 - 54.84 wt.%, SiO_2 0.61 - 3.35 wt.%, Al_2O_3 0.19 - 1.69 wt.%, Fe_2O_3 0.1 - 0.89 wt.%, TiO_2 <0.0003 - 0.08 wt.%, and MnO <0.01 - 9.186 wt%. Plotting of major oxide variation (x-axis) *versus* major oxide concentration of the sample on y-axis uses normalization from PAAS (Post-Archean Australian

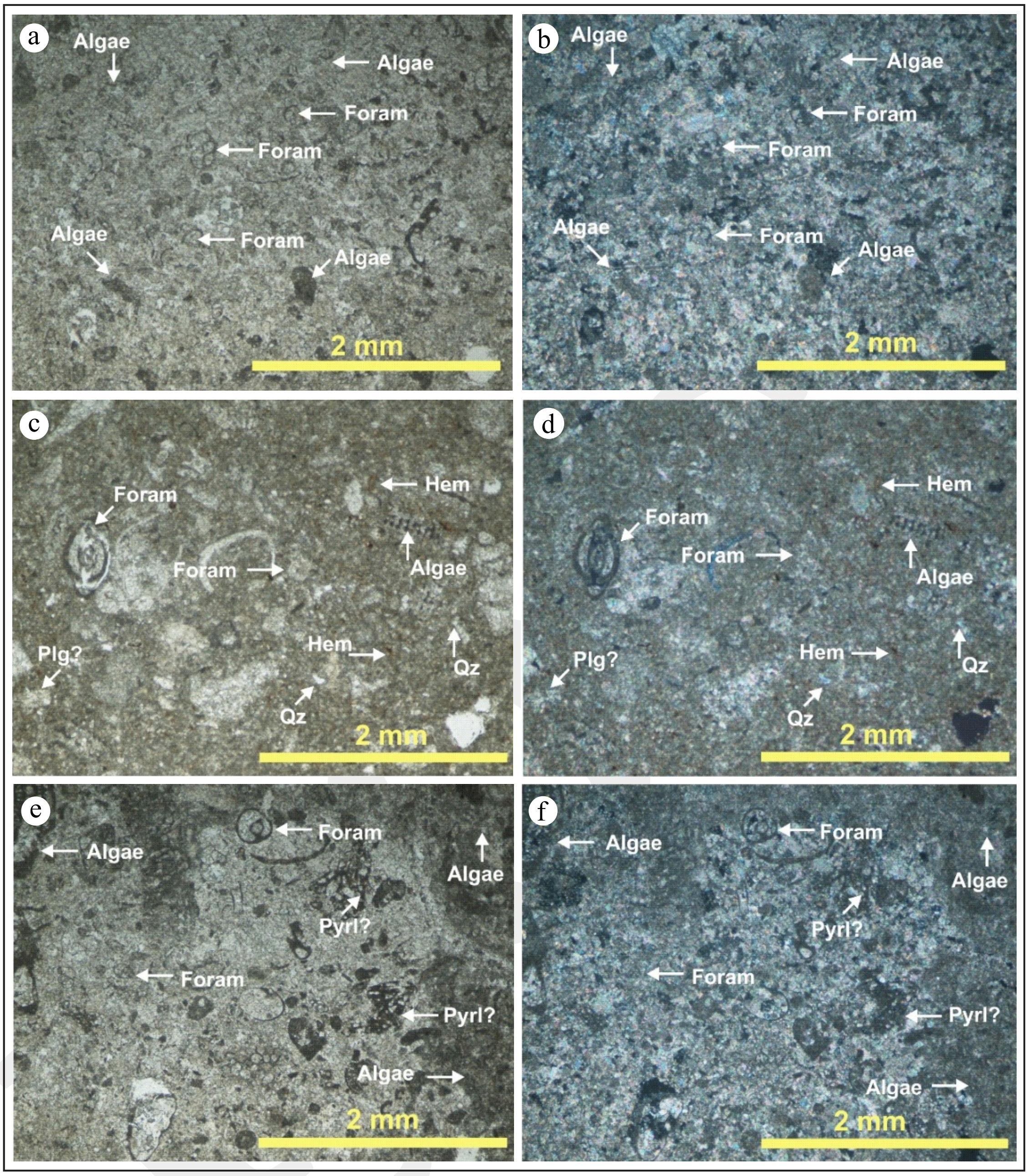

Figure 3. Photomicrographs of limestone: a) White limestone (PLW-2A) in plane polarized light (PPL) showing grains that are dominated by foraminifera and algae. b) White limestone (PLW-2A) in cross polarized light (XPL). c) Red limestone (PLR-2C) in plane polarized light (PPL) indicates an existence of impure minerals such as hematite, quartz, and plagioclase. d) Red limestone (PLR-2A) in cross polarized light (XPL). e) Grey limestone (PLG-5B) in plane polarized light (PPL) characterized by the presence of pyrolusite. f) Grey limestone (PLG-5B) in cross polarized light (XPL). Note: Foram = foraminifera; Qz = quartz; Pyrl = pyrolusite; Plg = plagioclase.

Shale; from Guimaraes *et al*., 2013). The plotting shows that CaO concentration of white limestone is the highest concentration of all limestone samples (Figure 4). The CaO concentration decreases from the white limestone to the coloured limestone (red or grey limestone). This trend is consistent with the results of petrographic identification and normative mineralogical calculation (Figure 3 and Table 3) showing the white limestone contains more abundant calcite ($CaCO_3$) of 95.48 wt. % (Table 3) in comparison with the red limestone which contains depleted calcite of 93.07 wt. % (Table 3) and impure minerals such as titanite ($CaTiSiO_5$), rodochrosite ($MnCO_3$), hematite (Fe_2O_3), feldspar,

Table 2. Trace and Rare Earth Element Concentration (ppm) in Limestone of Wonosari-Punung Formation, Ponjong Area, Gunungkidul Regency, Daerah Istimewa Yogyakarta

Rock	**White Limestone**	**Pink Limestone**	**Red Limestone**	**Light Grey Limestone**	**Grey Limestone**
Sample No	**PLW-2A**	**PLP-2B**	**PLR-2C**	**PLLG-5A**	**PLG-5B**
Cr	20	30	40	10	10
Mn	5018.48	9254.77	20290.78	26116.73	26154.78
Fe	437.15	2483.00	4766.66	6460.32	6749.76
Rb	0.2	0.4	0.4	0.3	0.2
Sr	445	159.5	235	137.5	116
Y	1.6	3.3	3.1	2.4	4.1
Zr	<2	<2	<2	2	2
Nb	<0.2	4.7	0.8	<0.2	<0.2
Ba	4.3	8.3	40	21.5	35
Cs	<0.01	0.01	0.01	0.04	<0.01
Ga	0.2	0.4	0.7	0.2	0.1
Hf	<0.2	<0.2	<0.2	<0.2	<0.2
Nb	<0.2	4.7	0.8	<0.2	<0.2
Sn	<1	<1	<1	<1	<1
Ta	<0.1	0.1	<0.1	<0.1	<0.1
Th	0.08	0.19	0.17	0.1	0.07
U	0.92	1.11	3.44	2.09	1.88
V	5	11	24	8	7
W	<1	<1	<1	<1	<1
La	0.8	2.3	1.9	1.1	1.3
Ce	0.6	2.5	2.1	1.2	1
Pr	0.14	0.47	0.38	0.22	0.24
Nd	0.7	1.9	1.8	1	1.1
Sm	0.12	0.41	0.48	0.28	0.25
Eu	0.07	0.12	0.12	0.08	0.07
Gd	0.22	0.4	0.46	0.26	0.37
Tb	0.03	0.06	0.06	0.04	0.05
Dy	0.18	0.37	0.41	0.29	0.36
Ho	0.05	0.08	0.08	0.05	0.08
Er	0.08	0.19	0.27	0.17	0.23
Tm	0.02	0.05	0.04	0.02	0.03
Yb	0.11	0.19	0.21	0.13	0.18
Lu	0.01	0.03	0.03	0.02	0.03
ΣREE	3.13	9.07	8.34	4.86	5.29

Table 3. Mineral Abundance in Limestone Samples of Wonosari-Punung Formation from Normative Mineralogical Calculation

Type of sample Mineral	**White limestone PLW-2A**	**Pink limestone PLP-2B**	**Red limestone PLR-2C**	**Light grey limestone PLLG-5A**	**Grey Limestone PLG5B**
	(wt.%)	**(wt.%)**	**(wt.%)**	**(wt.%)**	**(wt.%)**
Titanite	0.03	0.03	0.23	0.06	0.03
Hematite	-	0.16	0.51	-	-
Rhodochrosite	-	0.02	0.02	-	-
Feldspar (plagioclase)	0.62	0.94	2.50	< 1.25	< 0.73
Apatite	< 0.02	0.02	< 0.02	0.04	0.04
Dolomite	1.34	1.34	1.43	1.38	1.01
Siderite	0.07	-	-	0.19	0.14
Manganite/Pyrolusite	< 0.02	-	-	0.59	0.75
Calcite	95.48	95.37	93.07	95.19	93.97
Quartz	0.36	0.57	2.24	0.83	0.43
Total	97.94	98.45	100.02	99.53	97.1

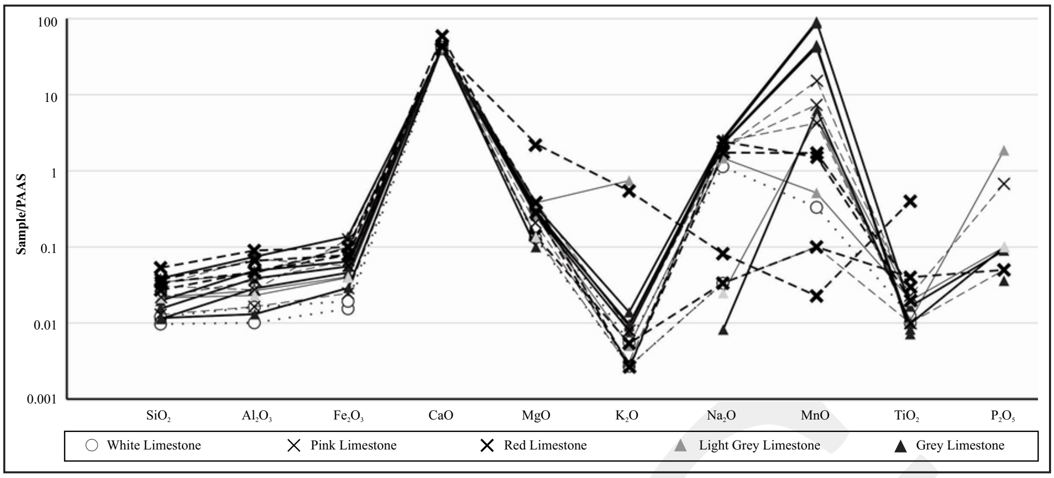

Figure 4. PAAS (Post-Archean Australian Shale) normalized major oxide diagram for limestone samples of Wonosari-Punung Formation. The PAAS normalizing factors are from Guimaraes *et al.* (2013).

and quartz. Additionally, the grey limestone contains depleted calcite (93.97 wt.%) in comparison with the white limestone and some impure minerals such as manganite ($Mn_2O_3.H_2O$) and/or pyrolusite (MnO_2) (Table 3). Therefore, this could suggest that the depletion of CaO concentration from the white limestone to the coloured limestone (red and grey limestone) is consistent with the colour changing on the limestone. In addition, Figure 4 presents that concentration of SiO_2, Fe_2O_3, and TiO_2 of the samples is increasing from the white limestone to the red limestone, and in the same way the concentration of MnO is increasing from the white limestone to the grey limestone. The rising up of the specific major oxide concentrations on the coloured limestones of red and grey limestone is consistent with the existence of impure minerals such as siderite ($FeCO_3$), rodochrosite ($MnCO_3$), titanite ($CaTiSiO_5$), hematite (Fe_2O_3), manganite ($Mn_2O_3.H_2O$), and/or pyrolusite (MnO_2) as seen on Figure 3 and Table 3. This tendency is also supported by mineralogical characteristics of some previous studies (Menezes, 2015; Titisari and Atmoko, 2015; Atmoko, 2016; and Atmoko *et al*., 2016).

The concentration of trace elements (Cr, Mn, Fe, Rb, Sr, Y, Zr, Nb, Ba, La, Ce, and Eu) including rare earth elements (REE) of the limestone samples increases from the white limestone to the red and grey limestones (Figures 5 and 6).

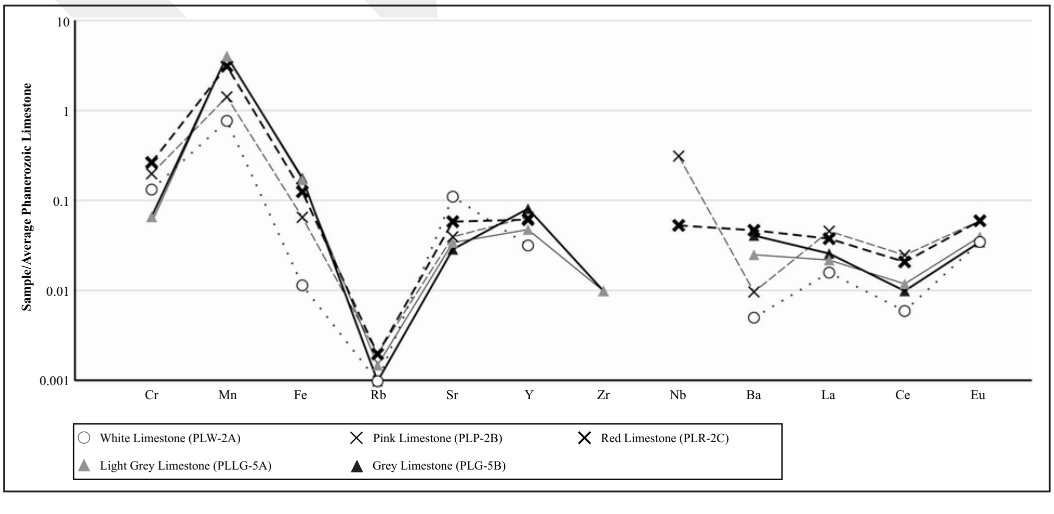

Figure 5. Average Phanerozoic Limestone-normalized trace elements diagram for limestone of Wonosari-Punung Formation. The Average Phanerozoic Limestone normalizing factors are from Condie *et al*. (1991).

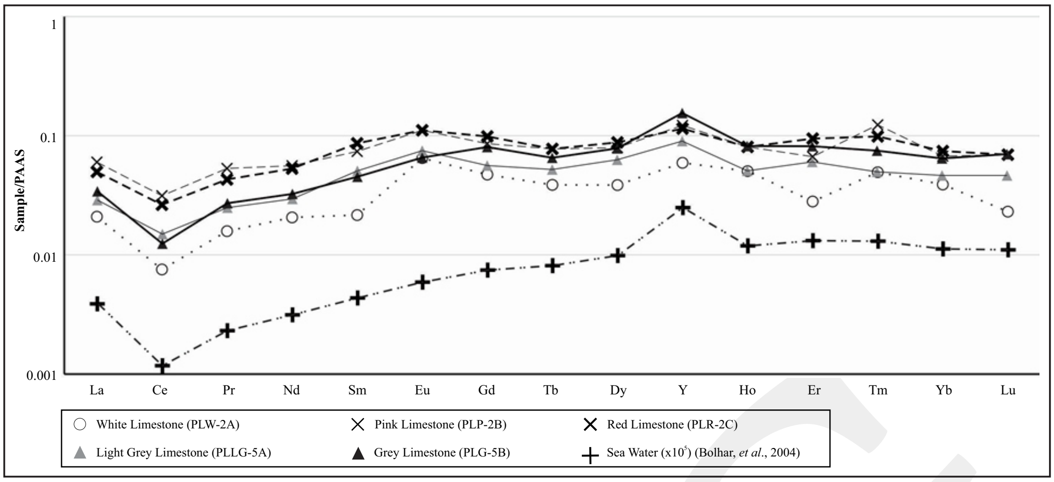

Figure 6. PAAS-normalized REE+Y diagram for limestone samples of Wonosari-Punung Formation. The PAAS normalizing factors are from Guimaraes *et al*. (2013).

Note that the plotting of normalized trace element and rare earth element concentrations is only performed on those five limestone samples from this study which are sample PLW-2A (white limestone), PLP-2B (pink limestone), PLR-2C (red limestone), PLLG-5A (light grey limestone), and PLG-5B (grey limestone). As has been mentioned before on the Analytical Method Section that trace element data from Menezes's study (2015) are not available. The rare earth element (REE) patterns for the various limestones vary consistently (Figure 6). However, all of the patterns in Figure 6 show depleted in light-REE (LREE) with respect to heavy-REE (HREE). All of the limestone samples exhibit negative cerium (Ce) anomalies and positive Yttrium (Y) anomalies. Moreover, enrichment of the normalized REE concentration for the white limestone to the coloured limestones shows a consistency with the enrichment of SiO_2, Fe_2O_3, TiO_2, and MnO concentrations from the white limestone to the coloured limestones (Figures 4 and 6). In addition, the pattern of the normalized rare earth element concentration of the limestone samples shows a consistency with seawater (Figure 6). Data of the seawater REE concentration is from Bolhar *et al*. (2004). The typical seawater REE profile is smooth and coherent with progressive enrichments in heavy REE with Ce negative anomaly and Y positive anomaly (Tostevin *et al*., 2016).

DISCUSSION

The plotting results of trace element (Cr, Mn, Fe, Rb, Y, Ba, La, Ce, and Eu) concentration of the limestone samples from this study exhibit enrichment trending from the white limestone to the red and grey limestone (Figure 5). In contrast, the Sr element shows the highest concentration in the white limestone and it decreases to the red and grey limestones (Figure 5). Azizi *et al*. (2014) and Nagendra and Nagarajan (2003) explained that Sr element depletion was an indicator of diagenetic process on limestone. According to Azizi *et al*. (2014), the concentration of Sr element in the Ching-dar limestone samples from Eastern Iran ranges from 121.14 to 191.13 ppm (mean = 159.12 ppm). The Sr values of these samples are less than that of their recent limestone counterpart, whereas in recent temperate carbonates it ranges from 1642 to 5007 ppm. The low content of Sr in comparison with recent limestone is mainly due to the removal by permeating freshwater during the diagenesis of these limestones. Therefore, the Sr depletion in the Ching-dar limestones was affected by meteoric diagenesis (Azizi *et al*., 2014). Similarly, according to Nagendra and Nagarajan (2003), Sr content from Shahabad limestone (Bhima Basin, India) varies from 121 ppm to 496 ppm showing the lower Sr content (121 ppm) that might be initially due to the influx of freshwater in the basin of deposition. Furthermore, it was accelerated by prolonged diagenesis in an open system under the influence of meteoric water (Nagendra and Nagarajan, 2003). This study shows Sr concentrations in the red and grey limestone samples range from 235 to 116 ppm (Table 2). The Sr concentrations of the coloured limestone samples are slightly similar to the Ching-dar limestones and the Shahabad limestone. Based on the Sr concentration in the Wonosari-Punung limestone samples and by referring to studies of Azizi *et al*. (2014) and Nagendra and Nagarajan (2003), it could be interpreted that the red and grey limestone samples of this study with lower Sr content (235 to 116 ppm) experienced more removal by freshwater during the diagenesis in comparison with the white limestone which is characterized by higher Sr content of 445 ppm. Involving freshwater on accelerating Sr depletion could suggest that the process of diagenesis might have occurred after the deposition of the limestone. Therefore, the Sr depletion of the coloured limestones suggests as an indicator of the diagenetic process occurring after the deposition of the limestones.

Profiles of REE concentrations in the limestone samples normalized by the PAAS (Post-Archaean Australian Shale) present a trend of the lowest value for the white limestone, and then the profiles show the increase in the grey and red limestones (Figure 6). According to Schieber (1988), possible co-precipitation of REE in carbonates from seawater is much too small to account for the REE enrichment. Therefore, only the diagenetic REE enrichment has to be considered. Referring to the study of Schieber (1988) and data of the REE enrichment profile of the limestone from the studied area (REE concentrations increase from the white limestone to the grey and then to the red limestone), consequently it could suggest that the diagenetic REE enrichment occurred on the white limestone and progressively to the grey and the red limestones.

The seawater REE profile which was reported by Tostevin *et al*. (2016) is consistent with the REE profiles of the limestone samples from the studied area which shows the trend of enrichment on heavy REE (Tb, Dy, Y, Ho, Er, Tm, Yb, and Lu) in respect to the light REE (La, Ce, Pr, Nd, Sm, Eu, and Gd) with Ce negative, slightly Eu positive, and Y positive anomalies (Figure 6). According to Tostevin *et al*. (2016), negative Ce anomalies preserved in carbonate sediments and rocks are a strong indication that the samples were precipitated in an oxic environment, and are abundant in most modern oxygenated waters. Therefore, conforming to Tostevin *et al*. (2016), increasing negative Ce anomalies from the white limestone to the coloured limestone on this study samples indicates an oxic condition that might be more intensive from the white limestone to the coloured limestone. This recognition is coherent to the interpretation of diagenetic processes on the limestone samples by freshwater which is progressive from the white to the coloured limestones and supported by Sr element depletion from the white to the coloured limestone.

Madhavaraju and Gonzáles-León (2012) explain that rare earth element data of limestone can be used to interpret depositional conditions. One of methods which is used to interpret limestone depositional conditions uses Mn* to determine the paleo-redox condition of limestone depositional environment. Machhour *et al*. (1994) and Bellanca *et al*. (1996) formulated Mn* as follow:

$$Mn^* = \log [(Mn_{sample}/Mn_{shale})/(Fe_{sample}/Fe_{shale})]$$

with Mn_{shale} and Fe_{shale} are 600 ppm and 46,150 ppm, respectively (Wedepohl, 1978).

The variations in the solubility of reduced manganese may lead to significant fractionation of these metals across the redox boundaries, where manganese tends to be incorporated under more oxygenated conditions above the redox boundary (*e.g*., Tribovillard *et al*., 2006; Madhavaraju and Lee, 2009; Piper and Calvert, 2009; Neumeister *et al*., 2016). Additionaly, a study of Madhavaraju and Lee (2009) shows that positive Mn* values indicate an oxic condition in limestone deposition.

The result of Mn* calculation from the Mn* formula on the limestone samples of Wonosari-Punung Formation generates Mn* value ranging between 2.457 - 2.946, and shows the positive values (Table 4). By referring to Madhavaraju and Lee (2009), it could be interpreted that the positive value of Mn* on the samples from the

Table 4. Elemental Ratios and Anomalies of Limestone of Wonosari-Punung Formation, Ponjong Area, Gunungkidul Regency, Daerah Istimewa Yogyakarta

Rock	Sample No	Mn*	Authigenic U	Ce/Ce*	Eu/Eu*	Y/Ho	La_N/Yb_N
White Limestone	PLW-2A	2.946	0.893	0.681	1.883	31.712	0.537
Pink Limestone	PLP-2B	2.457	1.047	0.623	1.391	40.879	0.894
Red Limestone	PLR-2C	2.515	3.383	0.800	1.200	38.401	0.668
Light Grey Limestone	PLLG-5A	2.493	2.057	0.741	1.394	47.568	1.394
Grey Limestone	PLG-5B	2.474	1.857	0.573	1.042	50.789	1.042

studied area suggests that the limestones were deposited in oxidative condition, and variation of the Mn* values possibly indicates the variety of oxidative condition in the limestone depositional environment.

The interpretations of the oxidative depositional condition can also be supported by authigenic U calculation with this formula: authigenic U = Total U - Th/3 (Wignall and Myers, 1988). Authigenic U calculations on the PLW-2A (white limestone), PLP-2B (pink limestone), PLG-5B (grey limestone), and PLLG-5A (light grey limestone) samples give result ranging from 0.893 to 2.057 (Table 4). According to Wignall and Myers (1988), the value of authigenic U, which is less or equal to 2, means that the limestone is deposited in oxidative condition. In contrast, the authigenic U concentration of PLR-2C (red limestone) samples is greater than 2, which are 3.383 (Table 4). The authigenic U concentration of the red limestone might be the indication of less oxidative conditions in comparison to the other limestone samples, or it shows a variation of oxidative condition during deposition. The authigenic U concentration of the limestone is consistent with the Mn* value, and it could be suggested an oxidative condition in the depositional environment of the limestone.

Rare earth element data of limestone can also be used to determine the source of the rare earth elements. Interpretation of rare earth element source can use Ce and Eu anomalies. Bau and Dulski (1996) and Bolhar *et al.* (2004) proposed Ce anomaly formula as follow: Ce/Ce* = Ce/(2Pr-1Nd). In oceanic water, Ce/Ce* values range from <0.1 to 0.4 (Elderfield and Greaves, 1982; Piepgras and Jacobsen, 1992), whereas in an average shale Ce/Ce* is 1 (Murray *et al*., 1991). According to Madhavaraju and Lee (2009) the Ce/Ce* value of below 1 is consistent with the negative Ce anomaly in the REE profile. Calculation of Ce/Ce* using the formula on the limestone sample from this recent studied area ranges from 0.573 to 0.800 (below 1; Table 4). According to Madhavaraju and Lee (2009), the Ce/Ce* values of the limestone samples which are below 1 indicates negative Ce anomalies (Figure 6). The negative Ce anomaly suggests that the main source of sediment is derived from the body of water as the result of precipitation (Madhavaraju and Gonzáles-León, 2012). In contrast, several studies have confirmed that positive Ce anomalies occur as the result of lithological input (*e.g.* Nath *et al*., 1992; Madhavaraju and Ramasamy, 1999). The Ce/Ce* of the limestone samples from the studied area (0.573 to 0.800) shows the value of below 1, but above 0.4 of oceanic water Ce/Ce* values. Therefore, this could suggest that there was an influence of the relative proportions of precipitation deriving from pure seawater and clastic contamination to the limestone depositional environment.

Madhavaraju and Lee (2009) mentioned a method to interpret the source of rare earth elements using Eu anomaly {$Eu/Eu^* = Eu_N/(0.5^*(Sm_N+Gd_N)$}. The calculation using the formula on the limestone samples of Wonosari-Punung Formation yields a result that Eu anomaly of the samples is ranging from 1.042 to 1.883 (Table 3). The value of Eu anomaly, which is more than 1, means that limestone has a positive Eu anomaly (Madhavaraju and Lee, 2009). Due to the result of Eu/Eu* on the limestone samples of the studied area (Table 4) showing more than 1, it indicates positive Eu anomalies. These positive Eu anomalies are shown by the REE plotting of PAAS-normalized on the limestone samples from this study (Figure 6). A positive Eu anomaly indicates that the limestone was affected by hydrothermal solutions (German *et al*., 1993; Kurian *et al*., 2008), intense diagenetic process (MacRae *et al*., 1992), plagioclase (feldspar) content (Nath *et al*., 1992), or input of aeolian sediment (Elderfield, 1988). In some cases, the terrigenous materials are characterized by the remain of plagioclase. The existence of feldspar (plagioclase) in the limestone samples, although in a very small quantity (Table 3, Figures 3c-d), shows a consistency with the positive Eu anomaly. The suggestion of the diagenetic process in the limestone depositional environment is supported by values of Sr concentration, Mn*, and authigenic U concentration The indication of contamination of terrigenous (clastic) materials in the limestone depositional environment is consistent with the suggestion of Ce/Ce* values. Both have been discussed in the previous discussion. Therefore, in relation to the positive Eu anomaly, the Eu/Eu* calculation, the presence of feldspar in the limestone samples from the studied area, then conforming to previous studies (German *et al*.,1993; Kurian *et al*., 2008; MacRae *et al*.,1992), it can interpret that rare earth elements in the limestone samples possibly were derived from a diagenetic process, terrigenous materials, and/or hydrothermal activity. Furthermore, the influence of the hydrothermal activity will be discussed later.

The interpretation of rare earth elements source could also be supported by the calculation of Y/Ho ratio and La_N/Yb_N ratio that were proposed by Bolhar *et al*. (2004). The calculation of the trace element ratios on the limestone samples from the studied area yields Y/Ho ratios from 31.712 to 50.789 and La_N/Yb_N ratios from 0.533 to 0.894 (Table 5). As terrestrial materials (i.e., felsic and basaltic crust) which have a constant Y/Ho ratio of ~ 26 and small admixtures of any contaminant, they would show seawater-like Y/Ho ratios of >44 (Bolhar, 2004). The Y/Ho ratios on the limestone from the studied area show a high ratio of Y/Ho or more than 26 (Table 5) by comparing to the Bolhar's ratios (2004). This can suggest that the limestone depositional environment was slightly contaminated by terrestrial material or had only small admixtures of any contaminant.

On the other hand, Madhavaraju and León (2012) mentioned that low La_N/Yb_N ratios of limestones from northeastern Sonora, Mexico, which are less than 0.1 were significantly lower than the values proposed by Condie (1991; about 1.0) and Sholkovitz (1990; about 1.3) for terrigenous materials. Therefore, the value of LaN/YbN ratios of limestone samples from the studied area which are slightly similar to La_N/Yb_N ratios of 0.5 - 1.04 (Table 5) with the proposed values of Condie (1991) and Sholkovitz (1990), indicates a contamination of terrigenous materials.

Carbonate in northern Sonora (Mexico), which shows the limestone, is having seawater-like REE+Y (Madhavaraju and León, 2012). According to them, this phenomenon suggests that the REE concentrations were mainly derived from seawater. A similar phenomenon of REE+Y pattern of the limestone from the studied area with the Sonora limestone shows a consistency with seawater pattern (Figure 6). However, the magnitude of REE concentration enrichment of the limestone in the studied area is much greater than the seawater. Therefore, it indicates the REE source of the limestone from the studied area was possibly derived from terrigenous (clastic) material contamination. The suggestion of terrigenous material input is supported by the positive Eu anomaly, the Eu/Eu* calculation, the Ce/Ce* values, Y/Ho ratios and La_N/Yb_N ratio, and the presence of feldspar in the limestone samples in the previous discussion. In relation to the geological condition of the studied area, the limestone units were deposited unconformably on the tuffaceous sandstone - calcareous sandstone unit (Figure 1b). It is possibly that the terrigenous materials were derived from the latter unit.

This following discussion is to continue interpretation of hydrothermal fluid activity that might be occurring on the limestone of the studied area. According to MacRae *et al*. (1992), German *et*

Table 5. Summary of Mineralogy and Geochemical Characterizations for Coloured Variety of the Limestones from the Wonosari-Punung Formation and Interpretation of the Limestone Depositional Environment and the Source of Trace Elements

	White limestone	**Grey limestone**	**Red limestone**	**Interpretation of limestone depositional environment and the source of trace element**
Mineralogy	Abundant of calcite	Manganite and pyrolusite as impure minerals	Hematite, quartz, feldspar (plagioclase), rhodochrosite, and titanite as impure minerals	
Major element (CaO)	The highest of Cao concentration	Depleted of CaO, enrichment of MnO	Depleted of CaO, enrichment of SiO_2, Fe_2O_3 and TiO_2	
	Depleted of CaO (calcite)			
Sr concentration	The highest of Sr concentration	Depleted of Sr concentration	Depleted of Sr concentration	
	Depleted of Sr			Diagenetic process, post depositional
REE concentration on REE profile	Depleted of REE concentration on REE profile			Oxidative condition
Mn*	Positive Mn* (2.95)	Positive Mn* (2.47)	Positive Mn* (2.52)	Oxidative condition
Authigenic U concentration	0.89	1.86	3.38	Oxidative condition
Negative Ce anomaly and Ce/Ce*	Negative Ce anomaly with Ce/Ce* of less than 1 (0.68)	Negative Ce anomaly with Ce/Ce* of less than 1 (0.57)	Negative Ce anomaly with Ce/Ce* of less than 1 (0.80)	Precipitation of sea water and clastic contamination
Positive Eu anomaly and Eu/Eu*	Positive Eu anomaly with Eu/Eu* of more than 1 (1.88)	Positive Eu anomaly with Eu/Eu* of more than 1 (1.04)	Positive Eu anomaly with Eu/Eu* of more than 1 (1.20)	Diagenetic process, contamination of terrigenous materials, and or hydrothermal fluid activity
Y/Ho ratio	High ratio of Y/Ho (31.71; more than 26)	High ratio of Y/Ho (50.79; more than 26)	High ratio of Y/Ho (38.40; more than 26)	Contamination of terrigenous materials
La_N/Yb_N ratio	Low La_N/Yb_N ratios (0.54; less than 1)	Low La_N/Yb_N ratios (1.04; less than 1)	Low La_N/Yb_N ratios (0.67; less than 1)	Contamination of terrigenous materials
Enrichment of Cr and Mn concentrations	Enrichment of Cr and Mn concentrations			Hydrothermal fluid activity

al. (1993), and Kurian *et al*. (2008), a positive Eu anomaly and Eu/Eu* value of limestone (more than 1) show one indication of three possibilities which are rare earth elements in the limestone deriving from the hydrothermal activity. By referring studies those three workers' studies and the data of the positive Eu anomalies and the Eu/Eu* values (above 1) of the limestone on the studied area, it tends to indicate that a hydrothermal activity occurred in the studied area. The indication is supported by Meyer *et al*. (2012) who mentioned that positive Eu anomalies might be present where seawater had mixed with hydrothermal fluids or indicated a hydrothermal vent source for marine waters present during deposition. Several data in the studied area that support a possibility of hydrothermal fluid activity in the limestone depositional environment are:

1. In this study, the sampling location is close to a fault (Figure 1a). Confirmed to Corbet and Leach (1977), geological structures (fault) could be a pathway for the rise of hydrother-

mal fluid to the earth surface. These data are supported by previous studies (Atmoko, 2016; Atmoko, *et al*., 2016) showing distribution of the red limestone which is located along the geological structure and their association with the activity of hydrothermal fluid.

2. The existence of silicified limestone (unmapped silicified limestone shown in Figure 1a), whereas the silicified rock is one of indications showing the activity of hydrothermal fluid worked in the area. Additionally, Hidayaturrahman (2008) reported the presence of silicified limestone in the studied area.
3. The existence of manganese deposit in Ponjong area, that has been reported by Menezes (2015), has supported the interpretation of the hydrothermal fluid activity in the studied area. This interpretation confirms a study of Butuzova *et al*. (1990) showing the genesis of manganese deposit in association with fluid hydrothermal activity.
4. The enrichment of Cr and Mn concentrations in the limestone samples taking place within the white limestone to the coloured limestone (Tables 1 and 2; Figures 4 and 5) is an indication of hydrothermal fluid activity in the studied area. This interpretation verifies a study of Meyer *et al*. (2012) mentioning that metal concentration enrichment of Cr and Mn could be an indication for depositional environment of the pink dolomite in relation to hydrothermal fluid activity.

The discussion of geochemical characterizations above for the various coloured limestone in the studied area, is summarized on Table 5. The table shows that the depletion of Sr concentration and the positive Eu anomaly (Eu/Eu* of more than 1) indicates a diagenetic process in the limestone depositional environment. This environment suggests an oxidative condition characterized by REE concentration profile, positive Mn*, and the value of the authigenic U. The oxidative condition of the limestone possibly occurred mainly after the deposition. The source of trace elements in limestone samples which is typified by the Ce/Ce* value of less than 1, the positive Eu anomaly (Eu/Eu* of more than 1), the high ratio of Y/Ho (more than 26), the low La_N/Yb_N ratios (less than 1), and the normalized high concentration of REE+Y patterns, was possibly derived from terrigenous (clastic) material input. The positive Eu anomaly and enrichment of Cr and Mn concentrations of the limestone are indications of hydrothermal fluid activity worked in the studied area. Based on the geochemical characteristics of the Punung-Wonosari limestone, therefore the depositional environment of the limestone was influenced by a combination of hydrothermal fluid activity with small amount of terrigenous material input and post depositional diagenetic process. The positive Eu anomaly might be an initiation of geochemical data for one of supporting data suggesting a possibility of hydrothermal fluid that has worked in the studied area. A further specific and comprehensive study will be necessary to be conducted for the topic of the hydrothermal fluids in the studied area. The summary of mineralogy and geochemical characterizations for the variety of limestone from the studied area and the interpretation of limestone depositional environment and the source of trace elements is shown in Table 5.

CONCLUSIONS

Limestone of Wonosari-Punung Formation in the studied area can be categorized into white limestone and coloured limestone of red and grey limestones. The colour of the limestones identifies their geochemical composition. The white limestone which contains more abundant calcite mineral ($CaCO_3$) in comparison with the red and grey limestones is characterized by the highest CaO concentration. The red limestone containing impure minerals such as quartz (SiO_2), rodochrosite ($MnCO_3$), hematite (Fe_2O_3), and titanite ($CaTiSiO_5$) is identified by depleted CaO but higher concentration of SiO_2, Fe_2O_3, MnO, and TiO_2. The grey limestone which contains manganite ($Mn_2O_3.H_2O$) and/or pyrolusite (MnO_2) performing as impure minerals is typified by depleted CaO and higher MnO. The limestone depositional environment on the studied area was influenced by a diagenetic process which is characterized by depletion of Sr concentration and the positive Eu anomaly (Eu/Eu* of more than 1). The depositional environment suggests an oxidative condition which is considered by REE concentration profile, positive Mn*, and the value of the authigenic U. The oxidative conditions of the limestone possibly occurred mainly after the depositional process. The positive Eu anomaly and enrichment of Cr and Mn concentrations of the limestone indicate that the hydrothermal fluid activity has been worked in the studied area. Characteristics of the limestone showing the value of Ce/Ce* (less than 1), the positive Eu anomaly (Eu/Eu* of more than 1), high ratio of Y/Ho (more than 26), low La_N/Yb_N ratios (less than 1), and REE+Y patterns suggest that the source of REE concentration of the limestone was derived from clastic material input. Therefore, the depositional conditions and source of rare earth elements of the Punung-Wonosari limestone on the basis of their geochemical characteristics were influenced by a combination of hydrothermal fluid activity with a small amount of clastic material input and post depositional diagenetic process.

ACKNOWLEDGMENTS

The authors would like to thank the Department of Geological Engineering, Faculty of Engineering, Universitas Gadjah Mada which has given funding for this study.

REFERENCES

Atmoko, D. D., 2016. *Depositional Environment and Mineral Controlling Red Limestone at Sawahan Area and surroundings, Ponjong Subregency, Gunungkidul Regency, Special Region of Yogyakarta (in Indonesian)*. Undergraduate Thesis at Dept. of Geological Engineering Faculty of Engineering, Universitas Gadjah Mada, 144pp.

Atmoko, D.D., Titisari, A.D., and Idrus, A., 2016. Mineralogy and Geochemistry of Ponjong Red Limestone, Gunungkidul, Daerah Istimewa Yogyakarta - Indonesia. *RISET - Geologi dan Pertambangan*, 26 (1), p.55-67. DOI: 10.14203/risetgeotam2016.v26.269

Azizi, S.H.H., Shabestari, G.M., and Khazaei, A., 2014. Petrography and geochemistry of Paleocene-Eocene limestones in the Ching-dar syncline, eastern Iran. *Geoscience Frontiers*, 5 (3), p.429-438. DOI: 10.1016/j.gsf.2013.08.002

Bau, M. and Dulski, P., 1996. Distribution of yttrium and rare earth elements in the Penge and Kuruman iron formation, Transvaal Supergroup, South Africa. *Precambrian Research*, 79 (1-2), p.37-55. DOI: 10.1016/0301-9268(95)00087-9

Bellanca, A., Claps, M., Erba, E., Masetti, D., Neri, R., Premoli-Silva, I., and Venezia, F., 1996. Orbitally induced limestone/marlstone rhythms in the Albian-Cenomanian Cismon section (Venetian región, northern Italy): sedimentology, calcareous and siliceous plankton distribution, elemental and isotope geochemistry. *Palaeogeography, Palaeoclimatology, Palaeoecology*, 126 (3-4), p.227-260. DOI: 10.1016/S0031-0182(96)00041-7

Berner, R.A., 1981. A new geochemical classification of sedimentary environments. *Journal of Sedimentary Petrology*, 51, p.359-365. DOI: 10.1306/212F7C7F-2B24-11D7-8648000102C1865D

Bodine, M.W., Holland, H.D., and Boresik, M., 1965. Co-Precipitation of manganese and strontium with calcite. *Symposium on problems of post magnetic ore deposition Praque,* 11, p.401-406.

Bolhar, R., Kamber, B.S., Moorbath, S, Fedo, C.M., and Whitehouse, M.J., 2004. Characterisation of early Archaean chemical sediments by trace element signatures. *Earth and Planetary Science Letters*, 222 (1), p.43-60. DOI: 10.1016/j.epsl.2004.02.016

Butuzova, G.Y., Drits, V.A., Morozov, A.A., and Gorschkov, A.I., 1990. Processes of formation of iron-manganese oxyhydroxides in the Atlantis-II and Thetis Deeps of the Red Sea. *Sediment-Hosted Mineral Deposits: Proceedings of a Symposium Held in Beijing,* *People's Republic of China*, 11, p.57-72. DOI: 10.1002/9781444303872.ch6

Chen, L., Lin, A.T.S., Da, X., Yi, H., Tsai, L.L.Y., and Xu, G., 2012. Sea-Level Changes Recorded by Cerium Anomalies in the Late Jurassic (Tithonian) Black Rocks Series of Qiangtang Basin, North-Central Tibet. *Oil Shale*. 29, p.18-35. DOI: 10.3176/oil.2012.1.03

Chien, N.X., Khai, P.N., Hien, D.T., Nguyen, D., Bot, D.C., Trung, T.V., Cuc, N.T., Minh, L.H., Thuc, N.V., Ngan, B.T., and Thuan, D.V., 2006. The Determination of rare earth elements in Geological and environmental samples by Inductively Coupled Plasma Mass Spectrometry. Institute for Technology of Radioactive and Rare Element. *The Annual Report* for 2006, VAEC, VAEC-AR 06-31, p.217-225.

Condie, K.C., 1991. Another look at rare earth elements in shales. *Geochimica et Cosmochimica Acta*, 55 (9), p.2527-2531. DOI: 10.1016/0016-7037(91)90370-K

Condie, K.C., Wilks, M., Rosen, D.M., and Zlobin, V.L., 1991. Geochemistry of metasediments from the Precambrian Hapschan series, eastern Anabar Shield, Siberia. *Precambrian Research*, 50 (1-2), p.37-47. DOI: 10.1016/0301-9268(91)90046-D

Coope, J.A., Lavin, O.P., Weiland, E.F., and James, L.D., 1991. *Exploration Geochemistry Short Course Manual*?

Corbett, G.J. and Leach, T.M., 1997. Southwest Pacific Rim Gold-Copper Systems: Structure, Alteration, and Mineralization. *Corbett Geological Services*, 318pp.

Elderfield, H., 1988. The oceanic chemistry of the rare earth elements. *Philosophical Transactions of the Royal Society of London*. 325, p.105-106. DOI: 10.1098/rsta.1988.0046

Elderfield, H. and Greaves, M.J., 1982. The rare earth elements in seawater. *Nature*, 296, p.214-219. DOI: 10.1038/296214a0

Embry, A.F. and Klovan, J.E., 1971. A Late Devonian Reef Tract on Northeastern Banks Island, NWT. *Canadian Petroleum Geology Bulletin*, 19, p.730-781.

German, C.R. and Elderfield, H., 1990. Application of Ce anomaly as a paleo redox indicator: the ground rules. *Paleoceanography*, 5, p.823-833. DOI: 10.1029/PA005i005p00823

German, C.R., Holliday, B.P., and Elderfield, H., 1993. A geochemical study of metalliferous sediment from the TAG hydrothermal mound, 26º08' N, Mid-Atlantic ridge. *Journal of Geophysical Research*, 98, p.9683-9692. DOI: 10.1029/92JB01705

Guimaraes, J.T.F., Cohen, M.C.L., Franca, M.C., Silva, A.K.T.D., and Rodrigues, S.F.S., 2013. Mineralogical and Geochemical Influences on Sediment Color from Amazon Wetlands Analyzed by Visible Spectrophotometry. *Acta Amazonica*, 43 (3), p.331-342. DOI: 10.1590/S0044-59672013000300009

Hidayaturrahman, H., 2008. *Penentuan umur batugamping tersilisifikasi dengan fosil foraminifera pada Daerah Sawahan, Kec. Ponjong, Kab. Gunung Kidul, Daerah Istimewa Yogyakarta.* Undergraduate thesis, Dept. Geological Engineering, Faculty of Engineering, Universitas Gadjah Mada, Unpublished, Yogyakarta.

Holser, W.T., 1997. Evaluation of the application of rare earth elements to paleoceanography. *Palaeogeography, Palaeoclimatology, Palaeoecology*, 132 (1-4), p.309-323. DOI: 10.1016/S0031-0182(97)00069-2

Jauhari, U. and Toha, B., 2005. High Resolution Sequence Stratigraphy and Diagenesis in Carbonate Rocks, Wonosari Formation, Yogyakarta: An Outcrop Analog for Modeling Chalky Limestone Reservoir Distribution. *Proceedings of Indonesian Petroleum Association, 30th Annual Convention & Exhibition, August 2005*. Indonesia.

Kurian, S., Nath, B.N., Ramaswamy, V., Naman, D., Gnaneshwar Rao., Kamesh Raju, K.A., Selvaraj, K., and Chen, C.T.A., 2008. Possible, detrial, diagenetic, and hydrothermal sources for Holocene sediments of the Andaman backarc basin. *Marine Geology*, 247 (3-4), p.178-193. DOI: 10.1016/j.margeo.2007.09.006

Lawrence, M.G. and Kamber, B.S., 2006. The behaviour of the rare earth elements during estuarine mixing - revisited. *Marine Chemistry*, 100 (1-2), p.147-161. DOI: 10.1016/j.marchem.2005.11.007

Liberatore, P.A., 1994. Determination of trace elements in geological samples by ICP AES. *ICP-AES Instrument at Work Varian*, ICP-16, 9p.

Liu, Y.G., Miah, M.R.U., and Schmitt, R.A., 1988. Cerium: a chemical tracer for paleo-oceanic redox conditions. *Geochimica et Cosmochimica Acta*, 52 (6), p.1361-1371. DOI: 10.1016/0016-7037(88)90207-4

Lokier, S.W., 1999. The Development of the Miocene Wonosari Formation, South Central Java. *Proceedings of Indonesian Petroleum Association, 27th Annual Convention & Exhibition. October 1999.* Indonesia.

Lokier, S.W., 1999. The Development of the Miocene Wonosari Formation, South Central Java. *Proceedings of Indonesian Petroleum Association, 27th Annual Convention & Exhibition. October 1999.* Indonesia.

Machhour, L., Philip, J., and Oudin, J.L., 1994. Formation of laminate deposits in anaerobic-dysaerobic marine environments. *Marine Geology*. 117 (1-4), p.287-302. DOI: Machhour, L., Philip, J., and Oudin, J.L., 1994. Formation of laminate deposits in anaerobic-dysaerobic marine environments. *Marine Geology*, 117, p.287-302.

MacRae, N.D., Nesbitt, H.W., and Kronberg, B.I., 1992. Development of a positive Eu anomaly during diagenesis. *Earth and Planetary Science Letters*, 109 (3-4), p.585-591. DOI: 10.1016/0012-821X(92)90116-D

Madhavaraju, J. and González-León, C.M., 2012. Depositional conditions and source of rare earth elements in carbonate strata of the Aptian-Albian Mural Formation, Pitaycachi section, northeastern Sonora, Mexico. *Revista Mexicana de Ciencias Geológicas*, 29, p.478-491.

Madhavaraju, J. and Lee, Y.I., 2009. Geochemistry of the Dalmiapuram Formation of the Uttatur Group (Early Cretaceous), Cauvery Basin, southeastern India: Implications on provenance and paleoredox conditions. *Revista Mexicana de Ciencias Geológicas*, 26, p.380-394.

Madhavaraju, J. and Ramasamy, S., 1999. Rare earth elements in limestones of Kallankurichchi Formation of Ariyalur Group, Tiruchirapalli Cretaceous, Tamil Nadu. *Journal of the Geological Society of India*, 54, p.291-301.

Medrano, M.D. and Piper, D.Z., 1992. A Normative-Calculation Procedure Used to Determine Mineral Abundances in Rocks from the Montpelier Canyon Section of the Phosphoria Formation, Idaho: A Tool in Deciphering the Minor-Element Geochemistry of Sedimentary Rocks. *U.S. Geological Survey Bulletin, 2023*, 32pp.

Menezes, A.M.B., 2015. *Geology and Characteristic Manganese Ore Deposit at Sambirejo Area, Sawahan Village, Ponjong Subregency, Gunungkidul Regency, Special Region of Yogyakarta (in Indonesian).* Undergraduate Thesis, Dept. of Geological Engineering, Faculty of Engineering, Universitas Gadjah Mada, Unpublished, Yogyakarta, 159pp.

Meyer, E.E., Quicksall, A.N., Landis, J.D., Link, P.K., and Bostick, B.C., 2012. Trace and rare earth elemental investigation of a Sturtian cap carbonate, Pocatello, Idaho: evidence for ocean redox conditions before and during carbonate deposition. *Precambrian Research,* 192 - 195 , p.89-106. DOI: 10.1016/j.precamres.2011.09.015

Morse, J.W. and Mackenzie, F.T., 1990. *Geochemistry of Sedimentary Carbonates*. Elsevier, New York, p.707. DOI: 10.1016/S0070-4571(08)70329-7

Mukti, M. M., Siregar, M. S., Praptisih, and Supriatna, N., 2005. Carbonate Depositional Environment and Platform Morphology of the Wonosari Formation in the Area East of Pacitan. *RISET - Geologi dan Pertambangan*, 15 (2), p.29-38. DOI: 10.14203/risetgeotam2005.v15.193

Murray, R.W., Ten Brink, M.R.B., Gerlach, D.C., Russ III, G.P., and Jones, D.L., 1991. Rare earth, major, and trace elements in chert-from the Franciscan complex and Monterey Group, California Assessing REE sources to fine grained marine sediments. *Geochimica et Cosmochimica Acta*, 55 (7), p.1875-1895. DOI: 10.1016/0016-7037(91)90030-9

Nagendra, R. and Nagarajan, R., 2003. Geochemical studies of Shahabad limestone (Younger

Proterozoic), Bhima Basin, Karnataka. *Indian Mineralogist*, 36 (1), p.13-23.

Nath, B.N., Roelandts, I., Sudhakar, M., and Plüger, W.L., 1992. Rare earth element patterns of the Central Indian Basin sediments related to their lithology. *Geophysical Research Letters*, 19, p.1197-1200. DOI: 10.1029/92GL01243

Neumeister, S., Algeo, T. J., Bechtel, A., Gawlick, H.J., Gratzer, R., and Sachsenhofer, R.F., 2016. Redox conditions and depositional environment of the Lower Jurassic Bächental bituminous marls (Tyrol, Austria). *Austrian Journal of Earth Sciences*, 109 (2), p.142-159. DOI: 10.17738/ajes.2016.0010

Northdurft, L.D., Webb, G.E., and Kamber, B.S., 2004. Rare earth element geochemistry of Late Devonian reefal carbonates, Canning Basin, Western Australia: Confirmation of seawater REE proxy in ancient limestones. *Geochimica et Cosmochimica Acta*, 68 (2), p.263-283. DOI: 10.1016/S0016-7037(03)00422-8

Piepgras, D.J. and Jacobsen, S.B., 1992. The behaviour of rare earth elements in seawater: precise determination of variations in the North Pacific water column. *Geochimica et Cosmochimica Acta*, 56 (5), p.1851-1862. DOI: 10.1016/0016-7037(92)90315-A

Piper, D.Z. and Calvert, S.E., 2009. A marine biogeochemical perspective on black shale deposition. *Earth Science Reviews*, 95 (1-2), p.63-96. DOI: 10.1016/j.earscirev.2009.03.001

Premonowati, Prastistho, B., and Firdaus, I. M., 2012. Allostartigraphy of Punung Paleoreef based on Lithofacies Distibutions, Jlubang Area, Pacitan Region-East Java. *Indonesian Journal of Geology*, 7 (1), p.113-122. DOI: 10.17014/ijog.v7i2.140

Schieber, J., 1988. Redistribution of rare-earth elements during diagenesis of carbonate rocks from the Mid-Proterozoic Newland Formation, Montana, USA. *Chemical Geology*, 69 (1-2), p.111-126. DOI: 10.1016/0009-2541(88)90163-5

Sholkovitz, E.R., 1990. Rare earth elements in marine sediments and geochemical standards. *Chemical Geology*, 88 (3-5), p.333-347. DOI: 10.1016/0009-2541(90)90097-Q

Siregar, M.S., Kamtono, Praptisih, and Mukti, M.M., 2004. Reef Facies of the Wonosari Formation, South of Central Java. *RISET - Geologi dan Pertambangan*, 14 (1), p.1-17.

Surono, Toha, B., and Sudarno, I., 1992. *Geological Map of the Surakarta-Giritontro Quadrangles, Jawa, 1408-3 and 1407-6 Quadrangles, Scale 1:100.000*. Research Centre and Geology Development. Department of Mining and Energy.

Titisari, A. D. and Atmoko, D.D., 2015. Genesis of Ponjong pink limestone, Gunungkidul, Special Region of Yogyakarta - Indonesia (in Indonesian). *Prosiding Seminar Nasional Kebumian ke-8 Jurusan Teknik Geologi, Fakultas Teknik, UGM. October 15 - 16, 2015*. Indonesia.

Toha, B., Purtyasti, R.D., Srijono, Soetoto, Rahardjo, W., and Pramumijoyo, S., 1994. Geology of Southern Mountain Area: A Contribution (in Indonesian). *Geology and Geotechnic Java Island, Since Late Mesozoic to Quarternary*, p.19-36.

Tostevin, R., Shields, G.A., Tarbuck, G.M., He, T., Clarkson, M.O., Wood, R.A., 2016. Effective use of cerium anomalies as a redox proxy in carbonate-dominated marine settings. *Chemical Geology*, 438, p.146-162. DOI: 10.1016/j.chemgeo.2016.06.027

Tribovillard, N., Algeo, T.J., Lyons, T., and Riboulleau, A., 2006. Trace metals as paleoredox and paleoproductivity proxies: An update. *Chemical Geology*, 232 (1-2), p.12-32. DOI: 10.1016/j.chemgeo.2006.02.012

Turekian, K.K., 1972. *Chemistry of the earth*. Holf, Rinechart and Winston, New York, NY. 131pp.

Wedepohl, K.H., 1978. Manganese: abundance in common sediments and sedimentary rocks. *Handbook of Geochemistry, II/3* (Wedepohl, K.H., ed), p.1-17, Springer.

Wignall, P.B. and Myers, K.J., 1988. Interpreting the benthic oxygen levels in mudrocks, a new approach. *Geology*, 16 (5), p.452-455. DOI: 10.1130/0091-7613(1988)016<0452:IBOLIM>2.3.CO;2